

We are IntechOpen, the world's leading publisher of Open Access books Built by scientists, for scientists

4,800

Open access books available

122,000

International authors and editors

135M

Downloads

Our authors are among the

154

Countries delivered to

TOP 1%

most cited scientists

12.2%

Contributors from top 500 universities



WEB OF SCIENCE™

Selection of our books indexed in the Book Citation Index
in Web of Science™ Core Collection (BKCI)

Interested in publishing with us?
Contact book.department@intechopen.com

Numbers displayed above are based on latest data collected.
For more information visit www.intechopen.com



Mechanisms of Significant Precipitation Hardening in a Medium Carbon Bainitic Steel by Complex Nanocarbides Composed of Nb, Ti and V

Makoto Okonogi, Takuya Hara and Hiromi Miura

Additional information is available at the end of the chapter

<http://dx.doi.org/10.5772/intechopen.80273>

Abstract

Precipitation-hardening behavior of various medium carbon bainitic steels with added elements of Nb, Ti and V was systematically investigated. Complex nanocarbides composed of Nb, Ti and V precipitated after aging in the steel with multiple additions of all the elements, whereas those with added individual elements were simple MC types. The amount of precipitation hardening (ΔH_v) after aging at 873 K of the former steel was approximately 90 ΔH_v , while those of the latter were less than 40 ΔH_v at best. Therefore, significant precipitation hardening took place by multiple element addition. The different amount of precipitation hardening depending on added elements was reasonably understood by considering misfit parameters between carbides and ferrite matrix.

Keywords: medium carbon steel, precipitation hardening, carbide, misfit parameter

1. Introduction

For machinery parts, such as bolts and gears, medium carbon steels are regularly employed. These steel parts are generally formed to prescribed shapes and designs through thermomechanical processes of hot and/or cold forging, and machining followed by heat treatments for further strengthening. Recently, demands for high strength steels, with their reduction of cost in addition to superior balance of mechanical properties, are increasing.

The dispersion of hard particles should be one of the most effective methods for strengthening. For this purpose, microalloyed steels with dispersed fine carbides are developed and actually employed for machinery parts because of their good balance of formability and strengthening

by heat treatment after the forming. It is reported that the dispersion of fine carbides such as VC, NbC, TiC and Mo₂C is effective for strengthening of low carbon ferritic and martensitic steels [1–3].

From the above background, some researches on precipitation-hardened medium carbon steels have been also undertaken. Murase et al. have investigated the precipitation-hardening behavior of medium carbon ferritic steels with single or multiple element additions of V and Cu [4] and have found that precipitation hardening of medium carbon steels is obviously improved by the multiple element addition of V and Cu rather than single additions of each element. Grange et al. precisely examined the effect of alloying elements (such as Mn, P, Si, Ni, Cr, Mo and V) on precipitation-hardening behavior in low and medium carbon steels with tempered martensite [5] and reported that the estimated hardening $H_{V_{\text{Estimated}}}$ could be evaluated by simple summation of the individual hardening effects as follows:

$$H_{V_{\text{Estimated}}} = H_V + \Delta H_{V_{\text{Mn}}} + \Delta H_{V_{\text{P}}} + \Delta H_{V_{\text{Si}}} + \Delta H_{V_{\text{Ni}}} + \Delta H_{V_{\text{Cr}}} + \Delta H_{V_{\text{Mo}}} + \Delta H_{V_{\text{V}}}, \quad (1)$$

where H_V and $\Delta H_{V_{\text{Mn}}}$, $\Delta H_{V_{\text{P}}}$, $\Delta H_{V_{\text{Si}}}$, $\Delta H_{V_{\text{Ni}}}$, $\Delta H_{V_{\text{Cr}}}$, $\Delta H_{V_{\text{Mo}}}$ and $\Delta H_{V_{\text{V}}}$ are the initial hardness of Fe–C alloy before element addition and the increments in hardness due to the individual element additions. On the other hand, Kosaka et al. investigated the precipitation-hardening behavior in 0.1 C–2.0 Mn steels (in mass %) with tempered martensite and revealed that the increase in precipitation hardening due to complex-composition carbide, that is, (Mo, V)C, is larger than those by carbides with simple compositions, that is, Mo₂C and VC [6]. They have also shown that the effect of carbides with simple compositions on hardening becomes larger in the order of Mo₂C, VC, TiC and NbC. The amount of precipitation hardening would be, therefore, considerably and complicatedly changed depending on the composition of carbide.

Medium carbon steels with bainite are well known for their good balance of mechanical properties of strength and ductility [7]. They are expected to be one of the most useful steels for machinery parts in the future. However, as far as the authors know, few studies on precipitation-hardening behavior and the strengthening mechanisms due to Nb, Ti and V additions in medium carbon steels with bainite have been carried out. Here, Nb, Ti and V are the most commonly employed elements for strengthening of low carbon steels as already shown above. In the present study, the effects of compositions of carbides on the precipitation-hardening behavior of medium carbon bainitic steel and the strengthening mechanisms are precisely investigated.

2. Experimental procedure

Various kinds of medium carbon steels with different compositions, shown in **Table 1**, were vacuum induction melted and cast into 15 kg ingots. Steel A is the base sample. In steels B, C and D, elements of Nb, Ti and V, respectively, were further added to the base sample. In steel E, Nb, Ti and V were all added. Mn as well as Mo was added to all the samples to attain bainite microstructure. The casted samples were then hot forged at 1523 K into bars with a diameter of 55 mm. The bars were solution treated at 1523 K for 30 min followed by air cooling down to

	C	Si	Mn	Mo	Ni	Nb	Ti	V	N	Fe
Steel A	0.26	0.69	1.59	0.50	0.35	—	—	—	0.003	Bal.
Steel B	0.26	0.71	1.59	0.49	0.35	0.019	—	—	0.003	Bal.
Steel C	0.26	0.70	1.58	0.49	0.35	—	0.039	—	0.003	Bal.
Steel D	0.25	0.71	1.58	0.49	0.35	—	—	0.30	0.003	Bal.
Steel E	0.25	0.71	1.58	0.49	0.35	0.020	0.038	0.31	0.003	Bal.

Table 1. Chemical compositions in mass% of tested medium carbon bainitic steels.

room temperature. Thereafter, some of the bars were aged for 120 min at various temperatures between 673 and 973 K.

Microstructural observations were carried out using optical microscopy and transmission-electron microscopy (TEM) on the cross-sections normal to the longitudinal direction of bars and at the positions of the half radius of the bars. Samples for the optical microscopic observation were prepared by mechanical polishing and etching using the nital solution of 3% nitric acid and 97% ethanol. TEM specimens were also prepared by mechanical polishing followed by electrolytic polishing using a solution of 5% perchloric acid and 95% acetic acid. The size, distribution and composition of precipitated carbides were examined by TEM equipped with energy-dispersive X-ray spectroscopy (EDS). The hardness was measured using a micro-Vickers hardness tester. The amount of precipitation hardening (ΔH_V) was estimated using the following equation:

$$\Delta H_V = (\text{Hardness after aging}) - (\text{Hardness before aging}) \quad (2)$$

3. Microstructure and hardness

Figure 1 shows the optical micrographs of the microstructure developed in steels D and E after solid-solution treatment at 1523 K for 30 min followed by air cooling, that is, before aging. It can be seen in **Figure 1** that a typical acicular bainite microstructure was almost uniformly evolved in both samples. A completely similar microstructure was observed to develop in all the other samples, while they are not displayed here.

The samples were then aged at various temperatures for 120 min and the change in the hardness was measured. **Figure 2** shows the summarized results of the amount of precipitation hardening (ΔH_V) as a function of aging temperature. In steels A, B and C, the maximum values of ΔH_V were approximately 30. This result indicates, therefore, precipitation hardening due to the additions of 0.019% Nb or 0.039% Ti (see **Table 1**) is quite small. On the other hand, the ΔH_V values in steels D and E after aging at 873 K exceeded 40. Moreover, in steel E, the maximum ΔH_V value was approximately 90. It should be noted, therefore, that the amount of precipitation hardening in steel E, $\Delta H_V = 90$, due to multiple element addition, is significantly larger than those in steels B, C and D with the single element additions. When the values of ΔH_V at 873 K are compared, it in steel E is larger than the summation of the ΔH_V values of

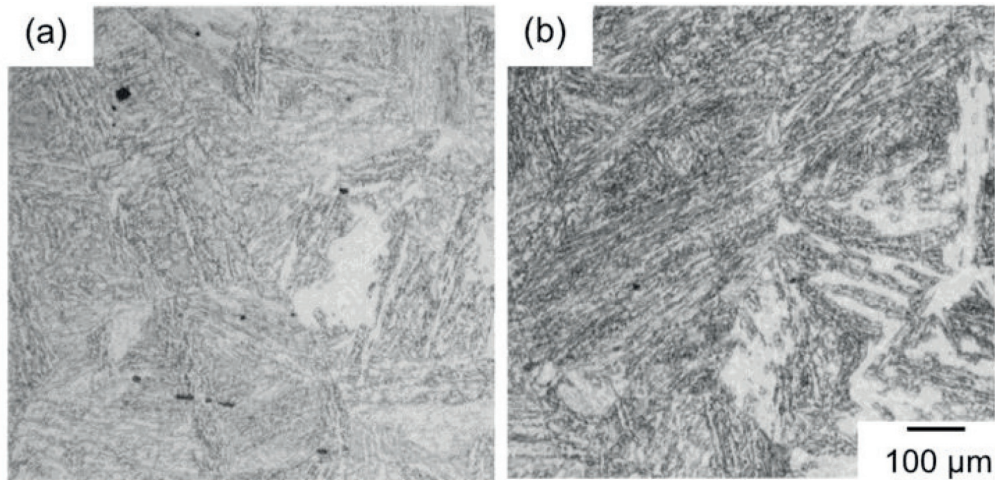


Figure 1. Typical microstructure of (a) steel D and (b) steel E after solution treatment at 1523 K for 30 min followed by air cooling.

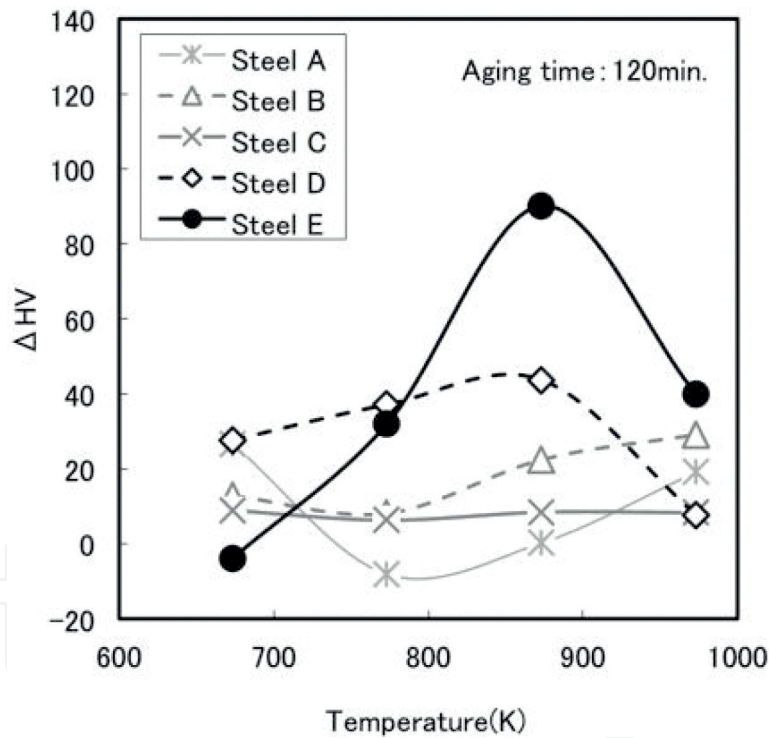


Figure 2. Change in the amount of precipitation hardening (ΔH_V) depending on aging temperature and added elements.

steels B, C and D, i.e., $\Delta H_V = 73$. This result indicates that the amount of age-hardening is not a simple summation of individual hardening as described in Eq. (1).

The developed precipitates were examined by TEM. **Figure 3** shows the typical TEM photographs of steels D and E after aging at 873 K for 120 min. In steel D, fine disk-shaped precipitates of 8 nm in diameter in average were distributed (**Figure 3(a)**). On the other hand, in

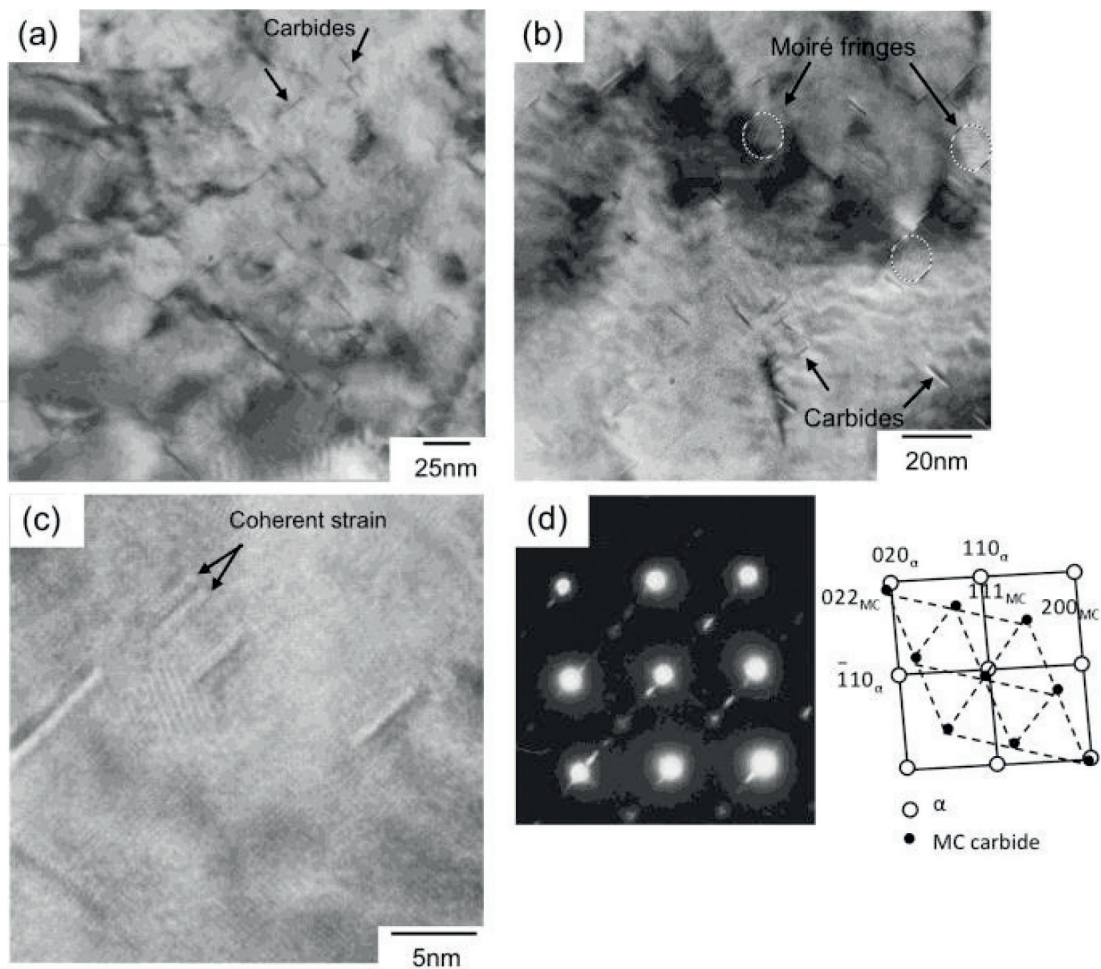


Figure 3. TEM micrographs of steels D and E after aging at 873 K: (a) Bright-field image of steel D, (b) Bright-field image of steel E, (c) magnified image of (b), and (d) diffraction pattern taken from the ferrite and MC carbide in (b).

steel E, slightly finer disk precipitates of approximately 5 nm in diameter were observed (**Figure 3(b)**). The size of precipitates in steel E looks more homogeneous than that in steel D. The moiré fringes due to the lattice misfit between the precipitates and matrix were also observed. High-resolution TEM observation of the precipitates in steel E revealed the presence of misfit strain at the edges of them indicating coherency of precipitate/matrix interface (**Figure 3(c)**). **Figure 3(d)** shows selected-area-diffraction pattern taken along direction parallel to the [001] axis of the matrix of steel E. Based on the analyses by the diffraction pattern and EDS, the fine precipitates were identified to be MC-type carbide having the Baker and Nutting crystallographic-orientation relationship, that is, $(100)_{MC} // (100)_{\alpha}$ $[010]_{MC} // [011]_{\alpha}$ and $[001]_{MC} // [011]_{\alpha}$ [8]. The EDS analysis indicated the compositions of carbides in steels D and E as VC and (Nb, Ti, V)C, respectively. Mo_2C carbides were not detected in all the samples.

It is reported that the critical size of MC-type carbides to keep coherency with matrix is approximately 5 nm and the loss of coherency derives a decrease in shear stress for dislocation to bypass the precipitates [3]. Even while the precipitates in steels A, B and C were not observed using TEM, the lower hardness of these steels than those of D and E (see **Figure 2**) should be affected by coherency loss of coarse MC-type carbides as observed in steel D.

4. Bypass mechanism and hardness

Precipitation-hardening behavior in medium carbon bainitic steels with added elements of Nb, Ti and V were precisely investigated. It was found that the amount of precipitation hardening became larger by the multiple element additions of Nb, Ti and V than the single addition of each element. Hardness changes due to change in dislocation bypass mechanism of particles. Even while hardness changes also depending on volume of the dispersed particles, the total amounts of particles contained in the present steels are assumed not largely different. The mechanisms of the change in the amount of precipitation hardening due to multiple element addition are precisely discussed below.

4.1. Dominant dislocation-bypass mechanism

There are two well-known mechanisms of dislocation to pass through particle at ambient temperature, that is, the Orowan [9] and the cutting mechanisms [10], which control threshold stress for dislocation motion in the particle-bearing materials. Their activation and role during plastic deformation change sensitively depending on precipitate size. Takaki has estimated the critical particle diameter for the cutting mechanism to be 7–10 nm at maximum for the MC-type carbides such as NbC, TiC and VC, whereas the Orowan mechanism can activate at ranges of 7–10 nm and over [11]. The precipitation size observed in the present study is approximately 5–8 nm in average (**Figure 3**).

When a gliding dislocation is pinned by a dispersed particle, the increase in the tensile stress ($\Delta\sigma$) can be expressed by the following equation [12, 13]:

$$\Delta\sigma = \beta Gb/\lambda \cdot \sin\theta, \quad (3)$$

where G is the shear modulus of matrix, b is the Burgers vector, λ is the mean particle spacing, θ is the bowing angle between the dislocation and the straight line that connects two particles, and β is a constant composed of Taylor's factor and the coefficient of shear stress, for which the value is approximately 3.2 [14]. The values of λ in steels D and E were measured by TEM observation to be 20 nm and 10 nm, respectively. The values of G and b are 80 GPa and 0.25 nm [14], respectively. Assuming that the tensile stress is empirically evaluated by one third of the hardness [13], the increase in the tensile stress ($\Delta\sigma$) of steels D and E can be estimated as 120 and 270 MPa, respectively, from their increase in hardness (ΔH_v) 40 and 90 by aging. Finally, the θ values in steels D and E can be calculated using Eq. (3) to be approximately 2.1 and 2.4°, respectively. These values are much smaller than those of particle/dislocation interaction by the Orowan mechanism, which shows a characteristic θ value of approximately 90° [12]. The Orowan mechanism should be, therefore, not activated as the dominant dislocation bypass mechanism in the present samples.

When the carbides were examined precisely by TEM, a typical contrast owing to coherent strain as well as Moiré fringe was observed (**Figure 3**). This indicates the presence of misfit strain due to interface coherency between carbides and matrix. Miura et al. have experimentally shown that dislocation passes through incoherent particles by the Orowan mechanism and coherent particles by cutting mechanism, and the latter deformation stress is higher than

the former one [15]. From the above arguments, the activated dislocation-bypass mechanism is concluded as a cutting mechanism irrespective of the present samples. The dominant dislocation bypass mechanism is closely related with the deformation stress [15]. However, it is revealed from the above argument that the bypass mechanism itself should not cause the change in hardness in the present samples. Nevertheless, according to the criteria proposed by Takaki [11], activation of the Orowan mechanism might be partially activated for such inhomogeneously and largely coarsen precipitates observed in **Figure 3(a)**.

4.2. Origin of higher hardness due to complex carbides

Gerold and Haberkorn have theoretically shown, considering the lattice misfit parameter at precipitate/matrix interface, that the increase in shear stress ($\Delta\tau_0$) due to dislocation detachment from precipitate is expressed by

$$\Delta\tau_0 = kG|\varepsilon|^{1.5} \left(\frac{fr}{b}\right)^{0.5}, \quad (4)$$

where k is a constant, f is the volume fraction of precipitates, r is the radius of the precipitate [10], ε is the lattice misfit parameter between the precipitate and matrix and ε is approximately 2/3 of the lattice misfit δ [16, 17]:

$$\varepsilon = \frac{2}{3} \delta, \quad (5)$$

and δ is expressed by

$$\delta = \frac{d_p - d_m}{d_m}, \quad (6)$$

where d_p and d_m are the lattice constants of precipitate and matrix, respectively [10]. Eq. (4) indicates that the shear stress ($\Delta\tau_0$) increases with increasing misfit parameter, size and volume fraction of precipitates.

The complex carbides of (Nb, V)C and (Ti, V)C are known to be continuous solid solution over the entire composition range [18]. The lattice constant d_p of the complex carbide such as (Nb, V)C, (Ti, V)C and (Nb, Ti, V)C is proportional to the composition and estimated by the following equation [19]:

$$d_p = \sum n_i d_i, \quad (7)$$

where i denotes the alloying element (i.e., Nb, Ti and V) to compose carbide, and n_i and d_i are the expediently estimated fraction of each carbide and the lattice constant, respectively. In the present study, d_p and d_m correspond to the lattice constants of $\{001\}_{MC}$ of carbide and of $\{011\}_\alpha$ of ferrite [8].

Change in the lattice misfit parameter between the matrix and carbide could be evaluated using Eqs. (5)–(7). The calculated misfit parameter (ε) of (Nb, V)C and (Ti, V)C is displayed

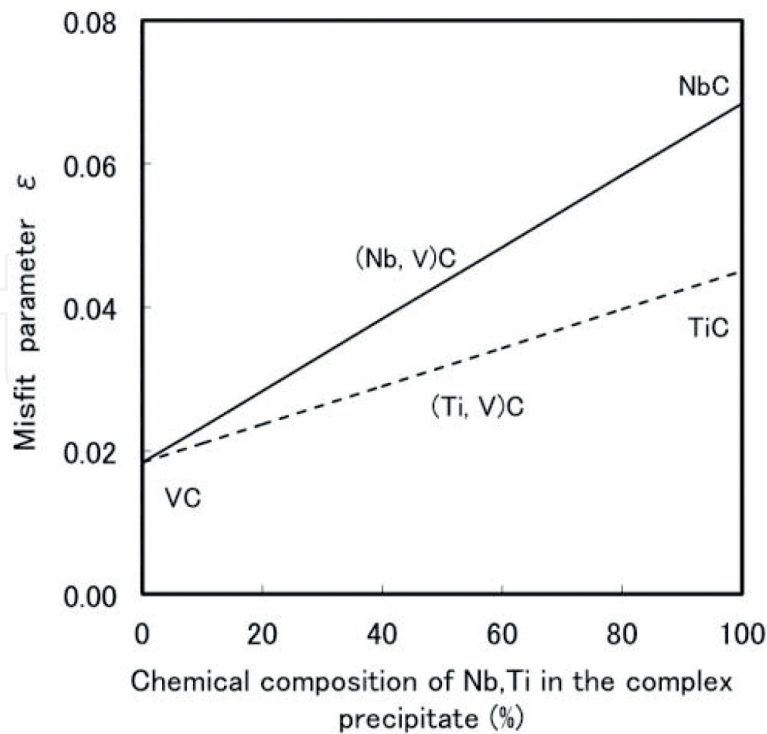


Figure 4. Calculated change in the lattice misfit parameter ε between matrix and complex precipitates of (Nb, V)C and (Ti, V)C depending on chemical composition.

in **Figure 4**. It is clear that the misfit parameter (ε) of the complex carbides (Nb, V)C and (Ti, V)C is larger than that of VC though smaller than those of NbC and TiC. Misfit parameter of (Nb, Ti, V)C complex carbide must be also linearly changed sensitively depending on the chemical composition.

In the same way, the lattice constant of (Nb, Ti, V)C complex carbide as well as the other carbides was determined. For this purpose, for an example of steel E, the chemical composition of the complex carbide at 873 K (i.e., aging temperature) was calculated to be (Nb_{0.03}, Ti_{0.12}, V_{0.85})C in atomic fraction by means of the "Thermo-Calc" software using the chemical composition in **Table 1**. **Figure 5** summarizes the calculated lattice misfit parameters (ε) of the carbides precipitated in the tested samples. It is evident that the misfit parameters (ε) of (Nb, Ti, V)C is greater than that of VC and smaller than those of NbC and TiC.

Miyamoto et al. have suggested that precipitation hardening (ΔH_V) due to carbides can be converted into increase in shear stress ($\Delta\tau_0$) by using the Taylor's factor of 2.08 in nontextured bcc metals by the following equation [20]:

$$\Delta\tau_0 = 3 \cdot \Delta H_V / 2.08, \quad (8)$$

Equation (8) indicates that the value of $\Delta\tau_0$ is proportional to precipitation hardening (ΔH_V). Actually, Ronay has investigated precipitation-hardening behavior in low carbon steels and shown a linear relationship between shear stress ($\Delta\tau_0$) and hardness (ΔH_V) due to TiN precipitation [21]. She also reported that the increase in the hardness and, therefore, shear stress due

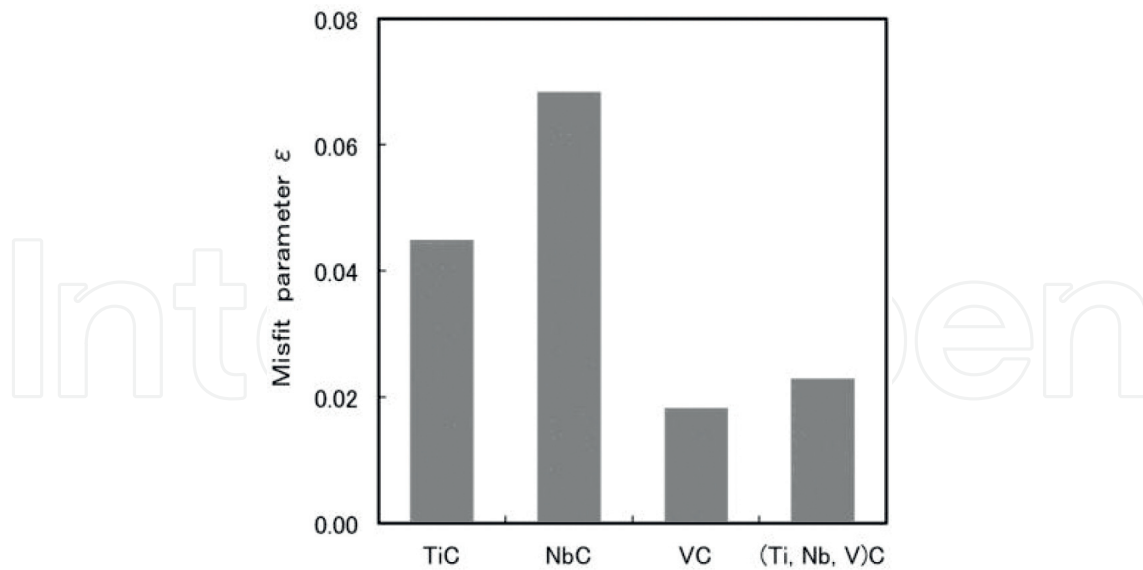


Figure 5. Comparison of the calculated lattice misfit parameter ϵ between matrix and precipitates of NbC, TiC, VC and (Nb, Ti, V)C.

to TiN precipitation could be reasonably understood by the quantitative estimation based on the cutting mechanism.

The amount of precipitation hardening (ΔH_v) of the tested samples can be estimated from Eqs. (4) and (7):

$$\Delta H_v = 0.69 \cdot kG|\epsilon|^{1.5} \left(\frac{fr}{b}\right)^{0.5}, \quad (9)$$

The constant k in Eqs. (4) and (9) is reported to be approximately 1–3 [22, 23]. The precipitation hardening (ΔH_v) by addition of 0.5 mass% Mo was quite small (**Figure 2**). Furthermore, Mo carbides were not detected by TEM observation in all the samples. From these reasons, the effect of Mo carbides on precipitation hardening can be excluded from the estimations. Therefore, carbides that mainly contribute to precipitation hardening in steels B, C, D and E are NbC, TiC, VC and (Nb, Ti, V)C, respectively.

Figure 6 shows the relationship between the measured ΔH_v values and the parameter $G|\epsilon|^{1.5} (fr/b)^{0.5}$ of the present steels. Calculated results using Eq. (9) and constant k of 1 and 3 are also shown by dotted lines. For the calculation of $G|\epsilon|^{1.5} (fr/b)^{0.5}$, the diameter of carbides ($2r$) was assumed to be 5 nm for simplicity, and the volume fraction of the precipitates (f) was estimated by the “Thermo-Calc” calculation using the chemical compositions in **Table 1**. It is evident in **Figure 6** that the results derived from experimental data of steels D and E appear between the lines with constant k of 1 and 3. The above results indicate that the values of ΔH_v calculated from Eq. (9) almost coincide with the present experimental data. That is, quantitative estimation of the amount of precipitation hardening (ΔH_v) in the medium carbon bainitic steels with Nb, Ti and V additions can be reasonably understood by the carbide/matrix lattice misfit parameter and cutting

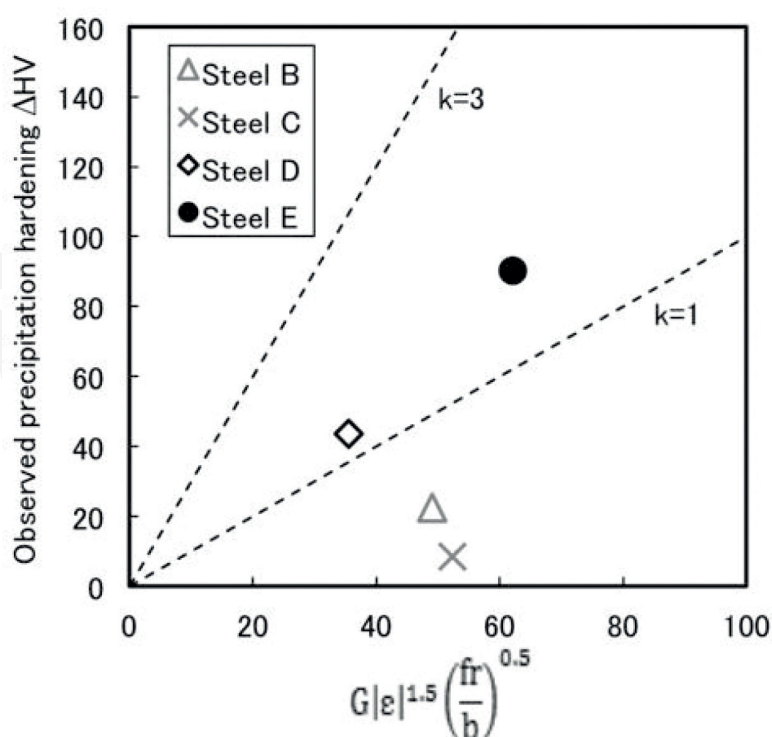


Figure 6. Relationship between the measured precipitation hardening (ΔH_V) and estimated parameter $G|\epsilon|^{1.5} (fr/b)^{0.5}$ using experimental data of the present steels, which are exhibited by symbols. For comparison, the relationship derived from Eq. (9) is also shown by dotted lines with k constants of 1 and 3.

mechanism for dislocation to pass through carbides. On the other hand, in steels B and C, the measured ΔH_V values were far from the calculated data. This could be because of the misfit dislocations that were produced around the carbides to reduce the misfit strain between carbides and matrix, since the misfit parameter (ϵ) of NbC and TiC is very large. Hence, precipitation hardening in steels B and C would not be understood simply by the cutting mechanism only presumably because of the loss of coherency between the coarsen carbides and matrix. Reduction of ΔH_V , therefore, took place because of a loss of coherency at the carbide/matrix interface [15]. Loss of coherency at the interface is well known to appear by coarsening [24, 25] and large lattice misfit strain [26]. Hence, complicated dislocation-bypass mechanisms could be activated depending on the size of precipitates in steels B and C.

5. Conclusions

The precipitation hardening due to complex carbides in medium carbon bainitic steels was investigated. The yielded results are as follows:

1. Small amount of additional elements can cause drastic change in the structures and chemical compositions of nanocarbides dispersed in steels, which induce conversion in dislocation bypass mechanisms to improve mechanical properties.

2. The amount of precipitation hardening in medium carbon bainitic steel with multiple element additions of Nb, Ti and V was larger than those in steels with single additions of these elements.
3. The dominant dislocation-bypass mechanism at room temperature of VC and (Nb, Ti, V)C carbides with a diameter approximately of 5–8 nm is the cutting mechanism, whereas that of NbC and TiC carbides appears different.
4. The difference in the amount of precipitation hardening could be reasonably understood by the lattice misfit parameter between carbide and matrix.
5. Cutting mechanism would not be dominant when the precipitate/matrix misfit parameter and size of carbides become large enough due to loss of coherency.

Acknowledgements

One of the authors, H.M., acknowledges the support by Japan Science and Technology Agency (JST) under Industry-Academia Collaborative R&D Program “Heterogeneous Structure Control: Towards Innovative Development of Metallic Structural Materials,” and the authors deeply appreciate this support.

Author details

Makoto Okonogi¹, Takuya Hara² and Hiromi Miura^{3*}

*Address all correspondence to: miura@me.tut.ac.jp

1 Kimitsu R&D Lab., Nippon Steel and Sumitomo Metal Corporation, Kimitsu, Chiba, Japan

2 Pipe and Tube Research Lab., Steel Research Laboratories, Nippon Steel and Sumitomo Metal Corporation, Amagasaki, Hyogo, Japan

3 Department of Mechanical Engineering, Toyohashi University of Technology, Toyohashi, Aichi, Japan

References

- [1] Funakawa Y, Shiozaki T, Tomita K, Yamamoto T, Maeda E. Development of high strength hot-rolled sheet steel consisting of ferrite and nanometer-sized carbides. *ISIJ International*. 2004;**44**:1945-1951. DOI: <https://doi.org/10.2355/isijinternational.44.1945>
- [2] Miyata K, Sawaragi Y. Effect of Mo and W on the phase stability of precipitates in low Cr heat resistant steels. *ISIJ International*. 2001;**41**:281-289. DOI: <https://doi.org/10.2355/isijinternational.41.281>

- [3] Miyata K, Omuma T, Kushida T, Komizo Y. Coarsening kinetics of multicomponent MC-type carbides in high-strength low-alloy steels. *Metallurgical Materials Transactions A*. 2003;**34**:1565-1573. DOI: <https://doi.org/10.1007/s11661-003-0303-x>
- [4] Murase Y, Iwase N, Takemoto Y, Senuma T. Precipitation hardening behavior of V and/or Cu bearing middle carbon steels. *Tetsu-to-Hagane*. 2013;**99**:669-675. DOI: <https://doi.org/10.2355/tetsutohagane.99.669>
- [5] Grange RA, Hribal CR, Porter LF. Hardness of tempered martensite in carbon and low-alloy steels. *Metallurgical Transactions A*. 1977;**8**:1775-1785. DOI: <https://doi.org/10.1007/BF02646882>
- [6] Kosaka M, Yoshida S, Tarui T. Precipitation hardening behavior of alloy carbide (Precipitation hardening and hydrogen trapping behavior in high strength steels-1). *CAMP-ISIJ*. 2004;**17**:1370. DOI: https://y100.isij.or.jp/acceptance/Ronbunzi/record_detail.php?-recid=18181
- [7] Takada H. Alloy designing of high strength bainite steels for hot forging. *Tetsu-to-Hagane*. 2002;**88**:534-538. DOI: https://doi.org/10.2355/tetsutohagane1955.88.9_534
- [8] Baker G, Nutting J. London, Iron and Steel Institute, Special Report. 1959;**64**:1-22. DOI: <https://trove.nla.gov.au/version/44983341>
- [9] Orowan E. Symposium on Internal Stresses in Metals and Alloys, Session III Discussion, Effects Associated with Internal Stresses. Institute of Metals, London; 1948. pp. 451-453. OCLC No.:1814639
- [10] Gerold V, Haberkorn H. On the critical resolved shear stress of solid solutions containing coherent precipitates. *Physica Status Solidi*. 1966;**16**:675-684. DOI: <https://doi.org/10.1002/pssb.19660160234>
- [11] Takaki S. Strengthening of steel by secondary particles. In: *Fundamentals and Applications of Precipitation in Steels*. Tokyo: Iron and Steel Institute of Japan; 2001. pp. 69-80. ISBN: 10:4930980267
- [12] Nakashima K, Futamura Y, Tsuchiyama T, Takaki S. Interaction between dislocation and copper particles in Fe-Cu alloys. *ISIJ International*. 2002;**42**:1541-1545. DOI: <https://doi.org/10.2355/isijinternational.42.1541>
- [13] Takahashi J, Kawasaki K, Kawakami K, Sugiyama M. Three-dimensional atom probe analysis of nitriding steel containing Cr and Cu. *Nippon Steel Technical Report*. 2005;**91**: 23-27. UDC 669.15'26'3-155.3:543.5
- [14] Nakashima K, Futamura Y, Tsuchiyama T, Takaki S. Precipitation strengthening at elevated temperature in Fe-Cu alloys. *Tetsu-to-Hagane*. 2003;**89**:524-529. DOI: https://doi.org/10.2355/tetsutohagane1955.89.5_524
- [15] Miura H, Tsukawaki H, Sakai T, Jonas JJ. Effect of particle/matrix interfacial character on the high-temperature deformation and recrystallization behavior of Cu with dispersed Fe particles. *Acta Materialia*. 2008;**56**:4944-4952. DOI: <https://doi.org/10.1016/j.actamat.2008.06.012>

- [16] Yeomans SR, McCormick PG. An investigation of precipitation and strengthening in age-hardening copper-manganese alloys. *Materials Science Engineering*. 1978;**34**:101-109. DOI: [https://doi.org/10.1016/0025-5416\(78\)90040-X](https://doi.org/10.1016/0025-5416(78)90040-X)
- [17] Takahashi J, Kawakami K, Kobayashi Y. Consideration of particle-strengthening mechanism of copper-precipitation-strengthened steels by atom probe tomography analysis. *Materials Science. Engineering A*. 2012;**535**:144-152. DOI: <https://doi.org/10.1016/j.msea.2011.12.056>
- [18] Hamar-Thibault S, Adnane L, Kesri R. Miscibility of binary VC–MC carbides in quaternary Fe–V–M–C alloys. *Journal of Alloys and Compounds*. 2001;**317-318**:311-314. DOI: [https://doi.org/10.1016/S0925-8388\(00\)01362-1](https://doi.org/10.1016/S0925-8388(00)01362-1)
- [19] Denton AR, Ashcroft NW. Vegard's law. *Physical Review A*. 1991;**43**:3161-3164. DOI: <https://doi.org/10.1103/PhysRevA.43.3161>
- [20] Miyamoto G, Hori R, Poorganji B, Furuhashi T. Interphase precipitation of VC and resultant hardening in V-added medium carbon steels. *ISI International*. 2011;**51**:1733-1739. DOI: <https://doi.org/10.2355/isijinternational.51.1733>
- [21] Ronay M. Nitridable steels for cold forming processes. *Metallurgical Transactions A*. 1981;**12**:1951-1955. DOI: <https://doi.org/10.1007/BF02643808>
- [22] Ibrahim IA, Ardell AJ. Hardening mechanisms in underaged ordered and disordered Cu₃Au-Co alloy single crystals. *Acta Metallurgica*. 1977;**25**:1231-1240. DOI: [https://doi.org/10.1016/0001-6160\(77\)90212-7](https://doi.org/10.1016/0001-6160(77)90212-7)
- [23] Ardell AJ. Precipitation hardening. *Metallurgical Transactions A*. 1985;**16**:2131-2165. DOI: <https://doi.org/10.1007/BF02670416>
- [24] Gerold V, Pham HM. Precipitation hardening by misfitting particles and its comparison with experiments. *Scripta Metallurgica*. 1979;**13**:895-898. DOI: [https://doi.org/10.1016/0036-9748\(79\)90182-0](https://doi.org/10.1016/0036-9748(79)90182-0)
- [25] Pande CS, Imam MA. Nucleation and growth kinetics in high strength low carbon ferrous alloys. *Materials Science. Engineering A*. 2007;**457**:69-76. DOI: <https://doi.org/10.1016/j.msea.2006.12.043>
- [26] Furuhashi T. Structure and energy of interphase boundaries in steel. *Tetsu-to-Hagane*. 2003;**89**:497-509. DOI: https://doi.org/10.2355/tetsutohagane1955.89.5_497

